



Originally published as:

Tanner, D. C., Krawczyk, C. (2017): Restoration of the Cretaceous uplift of the Harz Mountains, North Germany: evidence for the geometry of a thick-skinned thrust. - *International Journal of Earth Sciences*, 106, 8, pp. 2963—2972.

DOI: <http://doi.org/10.1007/s00531-017-1475-8>

# Restoration of the Cretaceous uplift of the Harz Mountains, North Germany: Evidence for the geometry of a thick- skinned thrust

**David C. Tanner** : *Leibniz Institute for Applied Geophysics, Stilleweg 2, 30655  
Hannover, Germany*

**Charlotte M. Krawczyk**: *Helmholtz Centre Potsdam, GFZ German Research Centre  
for Geosciences, Telegrafenberg, 14473 Potsdam, Germany; and  
TU Berlin, Ernst-Reuter-Platz 1, 10587 Berlin, Germany.*

## Abstract

Reverse movement on the Harz Northern Boundary Fault was responsible for the Late Cretaceous uplift of the Harz Mountains in northern Germany. Using the known geometry of the surface position and dip of the fault, and a published cross section of the Base Permian horizon, we show that it is possible to predict the probable shape of the fault at depth, down to a detachment level. We use the ‘inclined-shear’ method with constant heave and argue that a shear angle of  $30^\circ$  was most likely. In this case, the detachment level is at a depth of ca. 25 km. Kinematic restoration of the Harz Mountains using this fault geometry does not produce a flat horizon, rather it results in a ca. 4 km depression. Airy–Heiskanen isostatic equilibrium adjustment of the Harz Mountains restores the Base Permian horizon to the horizontal, as well as raising the Moho to a depth of 32 km, a typical value for northern Germany. Restoration also causes a rotation of tectonic fabrics within the Harz Mountains of about  $11^\circ$  clockwise. We show that this model geometry is very good fit to the interpreted DEKORP BASIN 9601 deep seismic profile.

# 1 Introduction

Despite the tremendous amount of geological and geophysical research that has been carried out on the Harz Mountains in northern Germany (Fig. 1), its structure at depth is still under debate, and a wide range of models have been put forward to explain its geological development. In particular, tectonic models of the Harz Mountains during the Late Cretaceous inversion phase have spanned thin- and thick-skinned, dip-slip thrusting to strike-slip models (Ruchholz 1983; Wrede 1988, 2008; Voigt et al. 2009), whereby the main consensus is dip-slip thrust movement on the Harz Northern Boundary Fault (HNBF) (Voigt et al. 2009).

The aim of this paper is to predict, using kinematic modelling, the likely geometry and detachment level of the HNBF in the lower crust. We also show results of the restoration of the Harz Mountains, i.e., kinematically restoring the Base Permian cutoffs to show the pre-deformation situation. We then carry out simple isostatic equilibrium and finally compare the model with the results of the DEKORP BASIN 9601 deep seismic profile (DEKORPBasin Research Group 1999; Krawczyk et al. 1999).

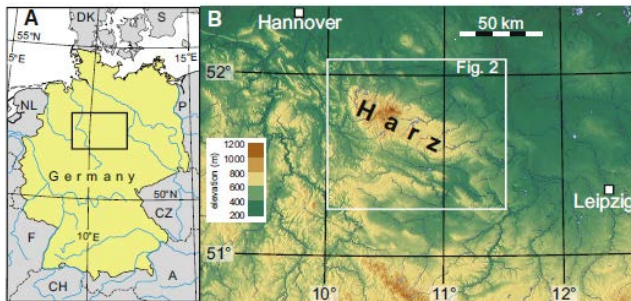


Fig. 1: A. Location of the Harz Mountains in Germany. B. Topographical elevation map of the Harz Mountains showing its prominence above the surrounding area and the clear radial drainage system of the rivers. Basemap taken from Braxmeir (1991).

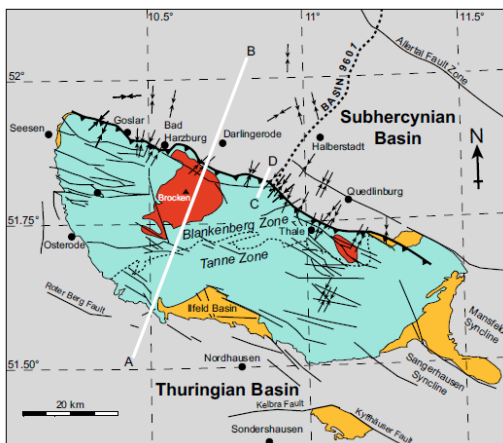


Fig. 2: Simplified geological map of the Harz Mountains, after Kley et al. (2008). Blue - Palaeozoic strata, orange - late Variscan sediments, grey - Mesozoic sediments, red - plutons. Fault lineaments are shown as black lines, important faults are named. The Harz Northern Boundary Fault is ornamented with triangles on the hanging-wall side of the thrust. The Subhercynian Basin is bounded to the north by the Allertal Fault Zone. Arrows indicate the direction of the maximum horizontal paleostress axes during the Late Cretaceous (data within the Harz Mountains from Franzke et al. (2007) and in the Subhercynian Basin from Brandes et al. (2013)). Cross-sections along lines A–B and C–D are shown in Figs. 3 and 4, respectively. Dashed line represents the trace of the DEKORP 9601 seismic profile (see Fig. 9).

## 2 Topography and geological setting

The Harz Mountains form a prominent topographic high in northern Germany. At the centre, it is ca. 500 m higher than the surrounding area (Fig. 1). Rivers radiate away from the centre, forming a major watershed between the River Weser and River Elbe to the west and east, respectively (Ersch and Gruber 1826). The topographic anomaly is approximately lozenge-shaped, NW–SE striking, ca. 95 km long and 35 km wide (Figs. 1, 2). In cross section (Fig. 3), the topographic shape is distinctly asymmetric, skewed to the north.

More than a 100 years ago, it was discovered that the Harz Mountains are entirely composed of strongly-cleaved, folded, and faulted Palaeozoic rocks that are surrounded on all sides by undeformed Mesozoic strata, i.e., it is a Palaeozoic outlier (Figs. 2, 3; Römer 1866, 1900). This was borne out by subsequent geological and geophysical work (e.g., Wrede 1988; Gabriel et al. 1996, 1997, 2001; Voigt et al. 2004, 2006; Brink 2011). The Harz Mountains form the most-northern outcrop of the Rhenohercynian Belt; the youngest sediments of the Harz Mountains are Carboniferous flysch and molasse that were sourced by the Variscan Orogeny (Engel et al. 1983). Subsequently, the whole European Permian Basin, which includes the Harz Mountains and the Subhercynian Basin, was buried by a thick cover of Latest Paleozoic to Mesozoic strata, until the Late Cretaceous, when inversion of the basin began (Littke et al. 2008).

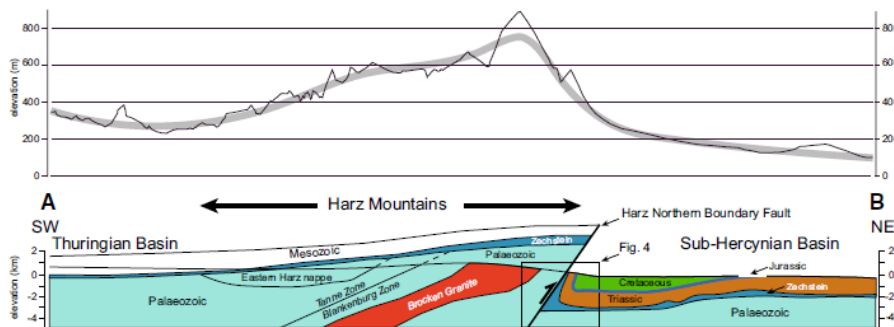


Fig. 3: Above: topographic elevation taken from Google Earth, grey line — moving average (window 500 m). Below: Simplified cross-section of the Harz Mountains, after Kley et al. (2008). Location of Fig. 4 is projected 15 km east. See Fig. 2 for location.

Four unconformities exist within Santonian to Campanian units in the Subhercynian Basin (SHB; Voigt et al. 2004, 2006), which lies directly to the north of the Harz Mountains (Fig. 2). Because the SHB was deformed as the Harz Mountains were thrust northward (Figs. 3, 4; Brandes et al. 2013), the unconformities precisely constrain the timing of fault activity and the uplift of the Harz Mountains to be between 85.8 and 71.3 Ma (von Eynatten et al. 2008), with respect to the latest stratigraphic information (Deutsche Stratigraphische Kommission 2012). These ages are reinforced by the fission-track- and (U-Th)/He cooling ages of zircon and apatite from the Harz Mountains and the SHB (von Eynatten et al. 2016), as well as by heavy mineral spectra from the SHB that record progressive erosion of the Mesozoic cover on the Harz Mountains (von Eynatten et al. 2008).

Detailed geological mapping and boreholes (see details in the following) have fixed the upper 1 km geometry of the HNBF, i.e., it dips by ca. 55° (Fig. 4; Franzke et al. 2004). The amount of throw on the fault has been estimated to be at least 6 km (Franzke et al. 2004). Note also that the Mesozoic beds of the SHB were strongly folded by the fault movement (Fig. 4).

Despite all the previous works, the complete shape of the fault and the exact depth of detachment (i.e., the point at which the fault is sub-horizontal in the crust) beneath the Harz Mountains are still unknown. For instance, various authors have suggested the HNBF detaches at depths of less than 10 km (Flick 1986), 10 km (Kley et al. 2008), or 18 km (Kley and Voigt 2008).

Paleo-stress indicators of the maximum stress direction during the Cretaceous inversion, as measured in the Harz Mountains and the SHB by Franzke et al. (2007) and Brandes et al. (2013), respectively, are overwhelmingly north-northeast–south-southwest oriented (Fig. 2). This is a good indication of the direction of thrusting during the Cretaceous (cf. Kockel 2003; Mazur et al. 2007), i.e., dip-slip movement on the HNBF. It also means that the cross-sectional lines in Figs. 2, 3, and 4 are in the tectonic transport direction.

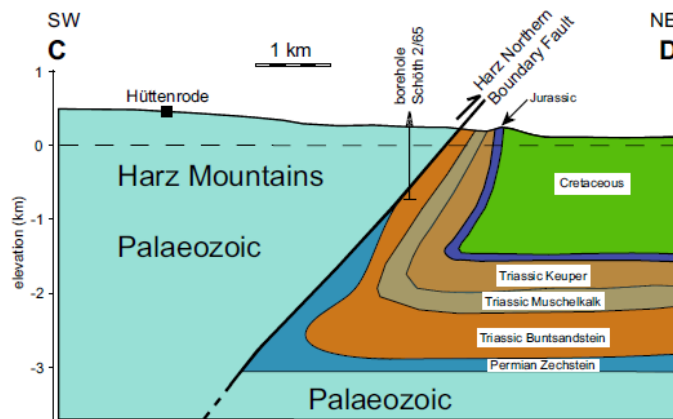


Fig. 4: Simplified cross-section of the northern boundary of the Harz Mountains near Hu'ttenrode. See Figs. 2 and 3 for location. Diagram modified after Franzke et al. (2004).

### 3 Methods

The steps carried out in this work were:

1. determining the depth geometry of the HNBF;
2. restoration of the Harz Mountains as the hanging-wall block of the HNBF, to the pre-Cretaceous situation;
3. isostatic re-equilibrium of the model.

#### 3.1 Predicting the geometry of the HNBF

Kinematic modelling, i.e., following the geometry of a fault's hanging wall, while it moves on the fault in question, allows the reverse process to be studied, i.e., the prediction of the fault geometry from the shape of the hanging wall (White et al. 1986). It is important to choose the most-adapt algorithm for modelling, that is one that will fulfill as many criteria as possible (White et al. 1986). For the study presented, we chose the 'inclined-shear' method (Groschong 2006). Other algorithms such as 'fault-parallel flow' or 'fault-bend folding' are inappropriate for models with fault cut-off angles above 40° (Ziesch et al. 2014; Brandes and Tanner 2014). A detailed description of the 'inclined-shear' method is given in the Appendix.

### 3.2 Restoration

The ‘inclined-shear’ restoration algorithm assumes that any changes in the angle of the fault are compensated by shear within the hanging wall, in the chosen shear direction (Groshong 1990). For a listric fault in which the fault angle decreases with depth, the movement vectors within the hanging-wall progressively change direction (Fig. 10). The amount of shear can be seen in the change in the angle of the movement vector (approximately 7°–8° between shear bands, see the Appendix). Because shearing takes place, bed length is not maintained (in fact, only lines in the shear direction do not change in length; Groshong et al. 2012).

Restoration here was carried out using the same ‘inclined-shear’ algorithm that was used for fault prediction. We chose the fault geometry that was predicted using a shear angle of 30° (see Fig. 5); the final model used for restoration is shown in Fig. 6. Restoration consisted of moving the hanging wall back along the fault plane until the hanging wall and footwall cutoffs of the Base Permian horizon matched.

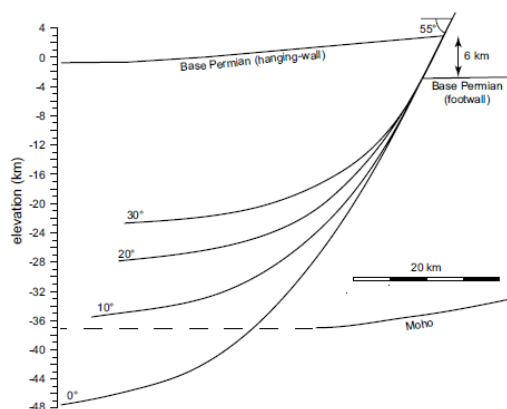


Fig. 5: Possible fault traces and depth to detachment predicted by the shape of the hanging-wall, using inclined shear with antithetic shear angles (see text) at 0, 10, 20, and 30°.

### 3.3 Airy–Heiskanen isostatic equilibrium

After restoration, the obtained model was equilibrated according to the Airy–Heiskanen principle of crustal buoyancy (Airy 1855; Heiskanen and Vening Meinesz 1958). This method assumes that the mass of an original column of crust, of thickness  $H$  and density  $\rho_c$ , is equal to the combined mass of a different column comprising: crust of thickness  $h_c$  and density  $\rho_c$  and mantle of thickness  $h_m$  and density  $\rho_m$  (Airy 1855). Therefore, the isostatic relationship is

$$(1) \quad \rho_c H = \rho_c h_c + \rho_m h_m.$$

Isostatic adjustment was carried out using densities for the crust and mantle of 2.9 and 3.3 g cm<sup>-3</sup>, respectively. These are typical density values for European lithosphere (Yegorova et al. 1995; Scheck et al. 1999).

If the surface mass is decreased by (tectonic) erosion, an appropriate vertical response is needed to equilibrate the model (Tsuboi 1978; Ménard et al. 1991), i.e., this means crustal uplift. The thickness of material removed ( $\Delta h$ ) is compensated by uplift which adds  $\Delta l$  thickness of mantle material to the base of the crust. After Tsuboi (1978),  $\Delta l$  is calculated using

$$(2) \quad \Delta l = (\Delta h \rho_c) / \rho_m.$$

We use the interpretation of the DEKORP 9601 seismic profile (DEKORP-Basin Research Group 1999; Krawczyk et al. 1999) for the position of Moho (ca. 35-37 km depth) beneath the Harz Mountains, compared to the typical depth of 30–33 km under the North German part of the European Permian Basin (Krawczyk et al. 1999). Unfortunately, the DEKORP profile does not extend under the Harz Mountains, so we have extended it as a dashed line in Figs. 5 and 6.

## 4 Results

### 4.1 Prediction of the geometry of the HNBF

Figure 5 shows the range of fault geometries that can be constructed for the known hanging-wall shape and the first kilometre depth of fault shape, using inclined shear at angles between  $0^\circ$  and  $30^\circ$ . Clearly, vertical shear ( $0^\circ$ ) is improbable, because the fault trace would have to penetrate the Mohorovičić discontinuity and continue into the mantle (Fig. 5). For the restoration modelling presented here, we chose a shear angle of  $30^\circ$ . The complete, present-day model, with all the elements used (i.e., the shapes of the internal zones of the Harz Mountains and the Brocken Granite, the fault, and the footwall/hanging-wall geometry), is shown in Fig. 6.

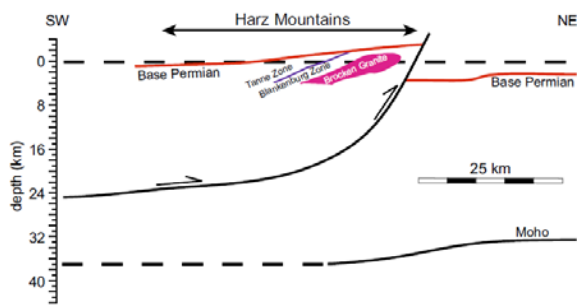


Fig. 6: Present-day cross-section of the Harz Mountains with detachment of the main thrust at ca. 25 km depth, as predicted by  $30^\circ$  inclined shear fault modelling.

### 4.2 Restoration

Restoration, i.e., restoring the hanging wall to its position before the Cretaceous event, so that the hanging wall and footwall cutoffs of the Base Permian horizon matched, causes two features. First, elements of the hanging wall rotate clockwise during the restoration by ca.  $11.5^\circ$  (Fig. 7). Therefore, the present-day steep dip of Variscan tectonic fabrics [i.e., steeply-dipping, NW-verging cleavage, and bedding (cf. Tanner et al. 2010)] within the Harz Mountains can be partly attributed to the Late Cretaceous compression. Second, the restored Base Permian horizon is not horizontal, and it dips both towards the HNBF from the south and north. The depression is ca. 4 km deep (Fig. 7).

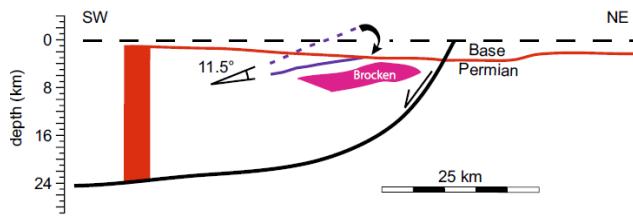


Fig. 7: Restoration of the Harz Mountains model to the Base Permian horizon using inclined shear. The dashed line represents the boundary between the Tanne and Blankenburg zones before restoration in Figure 6; the clockwise rotation angle of  $11.5^\circ$  is caused by restoration.

### 4.3 Airy–Heiskanen isostatic equilibrium

Calculation of the isostatic equilibrium adjustment was carried out using Eq. 2. For the peak height of the model after the Cretaceous event, i.e., at the fault (6 km), one obtains  $\Delta l$  of 5272 m, i.e., the model after restoration can be raised by this amount, which brings the Mohorovicic discontinuity at this position from 37 km to ca. 32 km depth (black line, Fig. 8). It also raises the Base Permian horizon to the horizontal (red line, Fig. 8). Since the listric fault raised the hanging wall by continually lesser amounts with distance from the fault, up to point around 50 km from the fault, where there was zero uplift, the amount of isostatic adjustment also decreases linearly to zero at this point (Fig. 6). The resulting isostatic uplift is represented as a triangle in Fig. 8. Calculating the isostatic adjustment of the SHB would require flexural isostasy; that is not the aim of this paper.

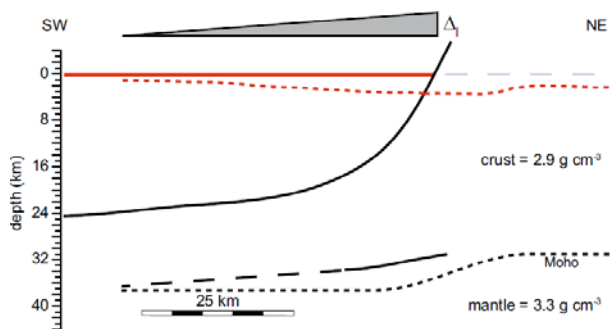


Fig. 8: Airy-Heiskanen isostatic equilibrium adjustment of the restored hanging-wall in Figure 7. Densities of the crust and mantle used in this work are shown. The triangle represents the amount of isostatic adjustment, where  $\Delta l$  is calculated using Eq. 2. Dashed and solid lines represent Moho (black) and the surface topography (red) in the model, before and after isostatic equilibrium, respectively.

## 5 Discussion

### 5.1 Fit of this model with the DEKORP BASIN 9601 deep seismic section

The final model, when placed within the DEKORP BASIN 9601 deep seismic section (DEKORP-Basin Research Group 1999; Krawczyk et al. 1999), shows that the detachment depth for the HNBF of ca. 25 km fits well with the interpreted detachment depths of the Haldensleben and Gardelegen Faults (Fig. 9; Krawczyk et al. 1999). Together, they form a foreland-propagating splay of emergent thrusts with a detachment level that rises,



from south to north, from a depth of 25–16 km. Best and Zirngast (1998, 1999) interpreted the BASIN 9601 seismic profile and identified many more south-dipping compressional faults between the HNBF and Gardelegen Fault, but with the same detachment level, as shown in Fig. 9.

Placing the Harz model in the DEKORP BASIN 9601 deep seismic section also raises two points, shown as A and B in Fig. 9. Reflectors below the point A probably represent short-cutting of the detachment from the Haldensleben Fault to the Gardelegen Fault. We envisage the following scenario: the Haldensleben Fault was first, and as the Gardelegen Fault developed, the higher branch point (at A) was less advantageous than the lower detachment propagating further north, where it joined the Gardelegen Fault at a more northerly point, thus creating the shortcut. The reflectors at point B are more enigmatic. Because they are at the same level (10–12 km depth) on both sides of the HNBF, this would point to their development being after the Upper Cretaceous event. We cannot speculate further on their relevance.

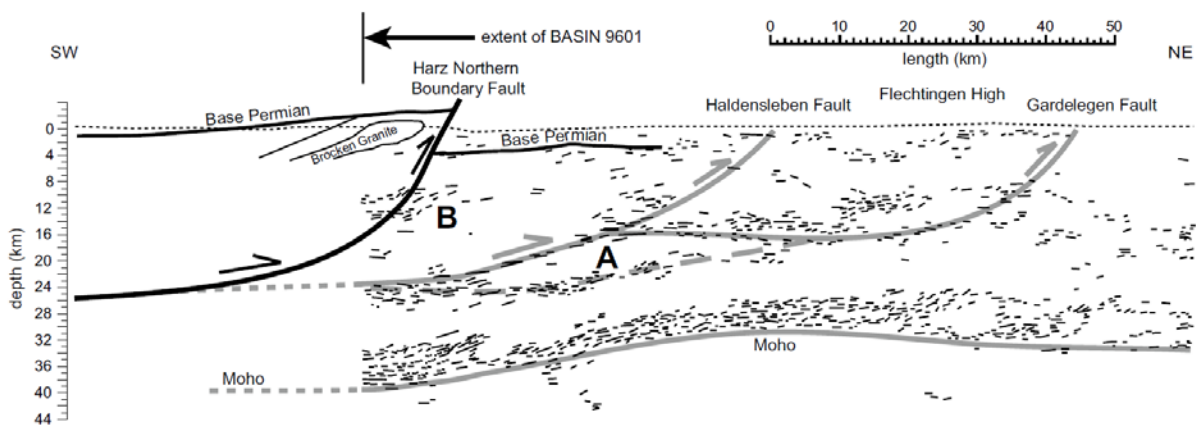


Fig. 9: The Harz model presented in this paper together with the line drawing of the DEKORP BASIN 9601 seismic section. The Harz structure fits well with the detachment depths of the Gardelegen and Haldensleben Faults, as interpreted in the seismic (DEKORP-Basin Research Group 1999; Krawczyk et al. 1999). Reflectors in areas A and B are discussed in the text.

Kossow and Krawczyk (2002) structurally balanced the BASIN 9601 profile and estimated the amount of deformation and erosion that occurred in the Northeast German Basin (NEGB) at the end of the Late Cretaceous. They discovered that the largest uplift of the Cretaceous/Tertiary unconformity (ca. 860 m), occurred at the southern margin of the seismic section, close to the Harz Mountains. Kossow (2002) estimated the detachment depth of the Gardelegen Fault (the major thrust directly to the north of the HNBF; Fig. 9). They found that a detachment depth of ca. 20 km best-fitted the shape of the hanging wall; thus, the model of Kossow (2002) substantiates the results shown here. Kossow and Krawczyk (2002) also suggest that the faults that are involved in the Late Cretaceous deformation were in fact previous normal faults of the NEGB.

We conclude from the detachment depth determined in this model that the detachment should, therefore, continue to the south at 25 km or deeper, to join the Bohemian Massif, the western border of which was also thrust to the north-west during the Late Cretaceous inversion phase (Tanner et al. 1998). Late Cretaceous inversion structures to the south of the Harz Mountains could be manifest either as thick or thinned-skinned structures, but should be still related to this lower crustal detachment. Proof of this may come from future deep seismic profiles in the German states of Thuringia and Saxony.

Kley and Voigt (2008) related the Late Cretaceous inversion phase in middle Europe to the effect of the convergence of Africa–Iberia–Europe, and not the Alpine collision. This caused the Pyrenean Orogeny, dated at ca. 85 Ma (Capote et al. 2002), and it was coeval with pulses of inversion or accelerated subsidence in many basins of the Iberian Peninsula (Reicherter and Pletsch 1991). This means that although this cross section of the Harz Mountains shown here is in the correct orientation (i.e., SW–NE), it is more than a thousand kilometres away from the Pyrenean collision. Kley and Voigt (2008) point out that this suggests efficient mechanical coupling of the lower crust during the Late Cretaceous, which was able to allow compressive stresses to extend this far northwest.

### ***5.2 The HNBF—an inverted normal fault?***

In many geodynamic situations, it is very common for normal faults, since they offer a zone of weakened crust, to be reactivated as reverse faults (e.g., McKenzie 1969; Sibson 1985; McClay 1989, 1995; De Paola et al. 2006). This phenomenon has even been recognised in unconsolidated glacial sands that were deformed by glacial isostatic adjustment (Brandes et al. 2012).

Because the coefficient of friction of natural rocks is around 0.85 (Bayerec 1977), compressive faults should have an angle of less than 30° (Anderson 1951; Sykes 1978). Because the HNBF has a dip of 55° at the Earth’s surface, we postulate that it was a normal fault that was active up to the Late Cretaceous when it was subsequently reactivated as a thrust. However, more detailed stratigraphic information is needed to clarify this point.

### ***5.3 The inclined-shear algorithm and the shear angle***

We deem the ‘inclined-shear’ algorithm to be the optimal method for this type of crustal model. The strongest criterion is that the cutoff angle of HNBF at the surface is greater than 50°. Other algorithms used to model compressional structures, for example, fault-parallel flow (Ziesch et al. 2014) or fault-bend folding (Suppe 1983; Medwedeff and Suppe 1997), assume that the faults have cut-off angles below 30°–35° (Brandes and Tanner 2014).

As shown in Fig. 5, the variable that, when using the inclined-shear algorithm, causes the greatest variation in fault geometry is the shear angle (Withjack and Peterson 1986). The appropriate shear angle has been discussed at length in the literature, for instance, Groshong (1989) suggested it should be exactly antithetic to the master fault. Other authors have suggested using the Coloumb angle of failure under the compressive stresses (Xiao and Suppe 1992), or the trend of second-order faults in the hanging wall (White et al. 1986). In addition, Hague and Gray (1996) showed that the commonest shear angle used in models is 30°.

Perhaps, the most-relevant evidence for this model of the Harz Mountains comes from Yamada and McClay (2003a, b), who took 60 cross sections through a 3D analogue sandbox model of an inverted half-graben with variable strike. In their model, the fault dip at the surface was greater than 60° and decreased to horizontal at the base of the sandbox, i.e., the fault was listric. The fault geometry was very similar to the fault shape presented in this work. For each section, they derived the appropriate shear angle to generate the fault geometry using the inclined-shear model in reverse, i.e., using the fault shape to predict the shear angle. The authors calculated that the apparent shear angle in all the sections was  $30^\circ \pm 15^\circ$  (Yamada and McClay 2003a).

All the above evidence points to a probable shear angle of  $30^\circ$  for the given model. The fit of the  $30^\circ$  shear-angle model to the DEKORP BASIN 9601 deep seismic profile, however, provides the best, independent evidence for the use of this particular shear angle.

## 6 Conclusions

We suggest the Late Cretaceous inversion event in Central Europe was thick-skinned (i.e. detachment in the lower crust at 25 km depth); for this reason, all the major faults that were involved in this deformation phase and reach the surface are widely spaced (tens of kilometres). With respect to this model and the interpretation of the DEKORP BASIN 9601 seismic profile, the deformation most likely propagated from southwest to northeast, as can be implied by the decrease in the depth of the detachment in this direction. We postulate that the HNBF was originally a Mesozoic normal fault that was inverted as a thrust during the Late Cretaceous.

## Acknowledgements

We acknowledge various discussions with colleagues about the Harz Mountains, especially Christian Brandes, Carl-Heinz Friedel, Bernd Leiss, and Axel Vollbrecht. Jonas Kley and Klaus Reicherter provided positive and comprehensive reviews. We thank Midland Valley Exploration for use of their Move software, which was used to carry out the restoration.

## Appendix

'Inclined-shear' fault prediction relies on knowledge of the initial fault dip and position, as well as the cutoffs of a certain horizon (Fig. 10). The method assumes constant heave on the fault over the whole fault length. The angle at which the hanging wall underwent shear during fault movement (known as the shear angle) must be estimated; in Fig. 10, the shear angle is  $30^\circ$  from the vertical, i.e., it dips at  $60^\circ$  towards the fault. The hanging-wall cutoff (A') is projected at the shear angle to the regional, i.e., the level of the footwall (point P). The horizontal length from P to A is  $q$ . At regular intervals of  $q$  from A, the points B, C, etc. are marked (Fig. 10). At each of the points, a shear construction line is projected to the hanging wall at the shear angle (points B'–G'). The lengths  $t_1$  to  $t_n$  are measured. The depth to the fault is calculated by projecting the shear construction lines downwards from the regional, using vectors  $t_1$  from A,  $t_1 + t_2$  from B,  $t_1 + t_2 + t_3$  from C, etc. (Grosong, 2006).

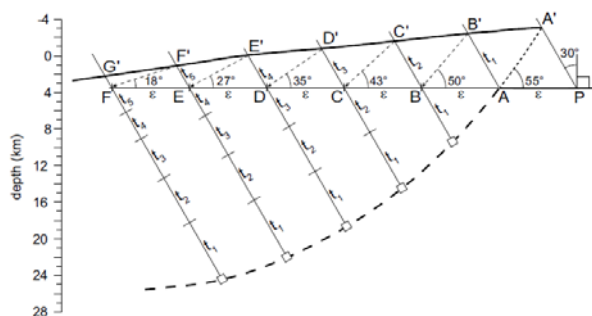


Fig. 10: The inclined-shear method to predict the shape of the fault using the hanging-wall geometry, the footwall/hanging-wall cutoffs and a specific shear angle, here  $30^\circ$ . Solid lines represent trace of Base Permian horizon, fine dashed thick line - known trace of the fault. Finely-dashed lines represent material vectors within the hanging-wall. The angle of the material vector from the horizontal is given.

## References

- Airy GB (1855) On the computation of the effect of the attraction of mountain masses, as disturbing the apparent astronomical latitude of stations in geodetic surveys. *Philos Trans R Soc* 145:101–104. doi:10.1098/rstl.1855.0003
- Anderson EM (1951) The dynamics of faulting and Dyke formation with applications to Britain. Oliver and Boyd, Edinburgh
- Bayerlee J (1977) Friction in rocks. In: Evernden JF (ed) Experimental studies of rock friction with application to earthquake prediction. U.S Geological Survey, Menlo Park, pp 55–77
- Best G, Zirngast M (1998) Die strukturelle Entwicklung der exhumierten Salzstruktur ‘Oberes Allertal’ Internal report of the Bundesanstalt für Geowissenschaften und Rohstoffe (BGR), ISBN 978-3-9813373-0-3
- Best G, Zirngast M (1999) Reconstruction of the exhumed upper Allertal salt structure. EGU Straßbourg 1999, J Conf Abstr 4:518
- Brandes C, Winsemann J, Meinsen J, Roskosch J, Tsukamoto S, Frechen M, Tanner DC, Steffen H, Wu P (2012) Activity along the Osning Thrust in Central Europe during the Lateglacial: ice-sheet and lithosphere interactions. *Quat Sci Rev* 38:49–62. doi:10.1016/j.quascirev.2012.01.021
- Brandes C, Schmidt C, Tanner DC, Winsemann J (2013) Paleostress pattern and salt tectonics within a developing foreland basin (north-western Subhercynian Basin, Northern Germany). *Int J Earth Sci* 102(8):2239–2254. doi:10.1007/s00531-013-0911-7
- Brandes C, Tanner DC (2014) Fault-related folding: a review of kinematic models and their application. *Earth Sci Rev* 138:352–370. doi:10.1016/j.earscirev.2014.06.008
- Braxmeir H (2011) SRTM-mission relief map. <http://www.maps-forfree.com>. Accessed 26 June 2016
- Brink H-J (2011) The crustal structure around the Harz Mountains (Germany): review and analysis. *Z Dt Ges Geowiss* 162(3):235–250. doi:10.1127/1860-1804/2011/0162-0235
- Capote R, Muñoz JA, Simón JL, Liesa C-L, Arlegui LE (2002) Alpine tectonics, I: the Alpine system north of the Betic Cordillera. In: Gibbons W, Moreno T (eds) *The geology of Spain*: London, The Geological Society of London, p 367–400
- DePaola N, Mirabella F, Barchi MR, Burchielli F (2006) Early orogenic normal faults and their reactivation during thrust belt evolution: the Gubbio Fault case study, Umbria-Marche Apennines (Italy). *J Struct Geol* 28:1948–1957. doi:10.1016/j.jsg.2006.06.002
- DEKORP-Basin Research Group (1999) Deep crustal structure of the northeast German Basin: new DEKORP BASIN 96 deep-profiling results. *Geology* 27:55–58. doi:10.1130/0091-7613(1999)027<0055:DCSOTN>2.3.CO;2
- Deutsche Stratigraphische Kommission, Menning M, Hendrich A (eds) (2012) *Stratigraphische Tabelle von Deutschland*. Deutsche Stratigraphische Kommission, Deutsches GeoForschungsZentrum, Potsdam
- Engel W, Franke W, Grote C, Weber K, Ahrendt H, Eder FW (1983) Nappe tectonics in the southeastern part of the Rheinisches Schiefergebirge. In: Martin H, Eder FW (eds) *Intracontinental fold belts*. Springer, Berlin, pp 267–288
- Ersch JS, Gruber JG (eds) (1826) *Allgemeine Encyclopädie der Wissenschaften und Künste*. FA Brockhaus, Leipzig
- Flick H (1986) The Hercynian mountains—a postorogenic overthrust massif? *Naturwissenschaften* 73(11):670–671. doi:10.1007/BF00366689
- Franzke H-J, Voigt T, von Eynatten H, Brix MR, Burmester G (2004) Geometrie und Kinematik der Harznordrandstörung, erläutert an Profilen aus dem Gebiet von Blankenburg. *Geowiss Mitt Thüringen* 11:39–62
- Franzke H-J, Müller R, Voigt T, von Eynatten H (2007) Paleo-stress paths in the Harz Mountains and surrounding areas (Germany) between the Triassic and the Upper Cretaceous. *Z geol Wissenschaft* 35(3):141–156
- Gabriel G, Jahr T, Jentzsch G, Melzer J (1996) The Harz Mountains, Germany: finite-element modeling of the evolution based on the interpretation of the gravity field. *Phys Chem Earth* 21(4):305–311. doi:10.1016/S0079-1946(97)00053-0
- Gabriel G, Jahr T, Jentzsch G, Melzer J (1997) Deep structure and evolution of the Harz Mountains: results of three-dimensional gravity and finite-element modeling. *Tectonophysics* 270:279–299. doi:10.1016/S0040-1951(96)00176-X
- Gabriel G, Jahr T, Weber U (2001) The gravity field south of the Harz Mountains: predominated by granitic material? *Z Geol Wiss* 29(3):249–266
- Groshong RH Jr (1989) Half graben structures: balanced models of extensional fault-bend folds. *Geol Soc Am Bull* 101(1):1329–1360. doi:10.1130/0016-7606(1989)101<0096:HGSBMO>2.3.CO;2
- Groshong RH Jr (1990) Unique determination of normal fault shape from hanging-wall bed geometry in detached half grabens. *Eclogae Geol Helv* 83:455–471. doi:10.5169/seals-166596
- Groshong RH Jr (2006) 3-D structural geology. A practical guide to quantitative surface and subsurface map interpretation, 2<sup>nd</sup> edn. Springer, Berlin. doi:10.1007/978-3-540-31055-6
- Groshong RH Jr, Withjack MO, Schlische RW, Hidayah TN (2012) Bed length does not remain constant during deformation: recognition and why it matters. *J Struct Geol* 41:86–97. doi:10.1016/j.jsg.2012.02.009
- Hague TA, Gray GG (1996) A critique of techniques for modelling normal-fault and rollover geometries. In: Buchanan PG, Niewland DA (eds) *Modern developments in structural interpretation, validation and modelling*. Geol Soc Lond Spec Pub 99:8997. doi:10.1144/GSL.SP.1996.099.01.08
- Heiskanen WA, Vening Meinesz FA (1958) *The earth and its gravity field*. McGraw-Hill, New York. doi:10.1017/S001675680006115X
- Kley J, Franzke H-J, Jähne F, Krawczyk C, Lohr T, Scheck-Wenderoth M, Sippel J, Tanner D, van Gent H, the SPP structural geology group (2008) Chapter 3.3—Strain and Stress. In: Littke R, Bayer U, Gajewski D, Nelskamp S (eds) *Dynamics of complex intracontinental basins—the Central European Basin System*, Springer, Berlin, pp 97–124. doi:10.1007/978-3-540-85085-4

- Kley J, Voigt T (2008) Late Cretaceous intraplate thrusting in central Europe: effect of Africa-Iberia-Europe convergence, not Alpine collision. *Geology* 36(11):839–842. doi:10.1130/G24930A.1
- Kockel F (2003) Inversion structures in central Europe—expressions and reasons, an open discussion. *Geol Mijnb* 82:367–382. doi:10.1017/S0016774600020187
- Kossow D (2002) Die kinematische Entwicklung des invertierten, intrakontinentalen Nordostdeutschen Beckens: Ergebnisse seismisch-stratigraphischer Untersuchungen und einer Profilbilanzierung. Dissertation, Deutsches GeoForschungsZentrum GFZ
- Kossow D, Krawczyk CM (2002) Structure and quantification of processes controlling the evolution of the inverted NE-German Basin. *Mar Pet Geol* 19:601–618
- Krawczyk CM, Stiller M, DEKORP-Basin Research Group (1999) Reflection seismic constraints on Paleozoic crustal structure and Moho beneath the NE German Basin. *Tectonophysics* 314:241–253. doi:10.1016/S0040-1951(99)00246-2
- Littke R, Bayer U, Gajewski D, Nelskamp S (2008) Dynamics of complex intracontinental basins: the central European basin system. Springer, Berlin, p 519. doi:10.1007/978-3-540-85085-4
- Mazur S, Scheck-Wenderoth M, Krzywiec P (2005) Different modes of Late Cretaceous-Early Tertiary inversion in the North German and Polish basins. *Int J Earth Sci* 94:782–798. doi:10.1007/s00531-005-0016-z
- McClay KR (1989) Analogue models of inversion tectonics. In: Cooper MA, Williams GD (eds) *Inversion tectonics*. *Geol Soc Lond, Spec Pub* 44, pp 41–59. doi:10.1144/GSL.SP.1989.044.01.04
- McClay KR (1995) The geometries and kinematics of inverted fault systems: a review of analogue model studies. In: Buchanan JG, Buchanan PG (eds) *Basin inversion*. *Geol Soc Lond Spec Pub* 88, pp 97–118. doi:10.1144/GSL.SP.1995.088.01.07
- McKenzie DP (1969) The relation between fault plane solutions for earthquakes and the directions of the principal stresses. *Bull Seismol Soc Am* 59:591–601
- Medwedeff DA, Suppe J (1997) Multibend fault-bend folding. *J Struct Geol* 19:279–292. doi:10.1016/S0191-8141(97)83026-X
- Ménard G, Molnar P, Platt JP (1991) Budget of crustal shortening and subduction of continental crust in the Alps. *Tectonics* 10:231–244. doi:10.1029/90TC02552
- Reicherter KR, Pletsch TK (2000) Evidence for a synchronous circum-Iberian subsidence event and its relation to the African-Iberian plate convergence in the Late Cretaceous. *Terra Nova* 12:141–147. doi:10.1046/j.1365-3121.2000.00276.x
- Römer FA (1866) Beiträge zur geologischen Kenntniss des norddeutschen Harzgebirges. 5. Abtheilung Palaeontogr 13(5):201–236
- Römer FA (1900) Beiträge zur geologischen Kenntniss des nordwestlichen Harzgebirges. *Palaeontogr* 1(9):1–46
- Ruchholz K (1983) Bretonischer Blattverschiebungsmechanismus im Harz und seine Bedeutung im Bereich des Rhenischen Troges. *Thesen Koll, Zentralinst Physik der Erde*: 1–8
- Scheck M, Barrio-Alvers L, Bayer U, Götze H-J (1999) Density structure of the Northeast German basin: 3D modelling along the DEKORP line BASIN 96. *Phys Chem Earth Part A Solid Earth Geod* 24(3):221–230. doi:10.1016/S1464-1895(99)00022-8
- Sibson RH (1985) A note on fault reactivation. *J Struct Geol* 7:751–754. doi:10.1016/0191-8141(85)90150-6
- Suppe J (1983) Geometry and kinematics of fault-bend folding. *Am J Sci* 283:684–721. doi:10.2475/ajs.283.7.684
- Sykes LR (1978) Intraplate seismicity, reactivation of preexisting zones of weakness, alkaline magmatism, and other tectonism post-dating continental fragmentation. *Rev Geophys* 16(4):621–687. doi:10.1029/RG016i004p00621
- Tanner DC, Behrmann JH, Oncken O, Weber K (1998) Three-dimensional retro-modelling of transpression on a linked fault system: the Upper Cretaceous deformation on the western border of the Bohemian Massif, Germany. In: Holdsworth RE, Strachan RA, Dewey JF (eds) *Continental transpressional and transtensional tectonics*. *Geol Soc Lond Spec Publ* 135, pp 275–287. doi:10.1144/GSL.SP.1998.135.01.18
- Tanner DC, Brandes C, Leiss B (2010) Structure and kinematics of an outcrop-scale, fold-cored triangle zone. *Bull Am Assoc Pet Geol* 94(12):1799–1809. doi:10.1306/06301009188
- Tsuboi C (1983) *Gravity*. George Allen and Unwin, London 254 pp
- Voigt T, von Eynatten H, Franzke H-J (2004) Late Cretaceous unconformities in the Subhercynian Cretaceous Basin (Germany). *Acta Geol Pol* 54:673–694
- Voigt T, Wiese F, von Eynatten H, Franzke H-J, Gaupp R (2006) Facies evolution of syntectonic Upper Cretaceous deposits in the Subhercynian Cretaceous basin and adjoining areas (Germany). *Z Dt Ges Geowiss* 157:203–244. doi:10.1127/1860-1804/2006/0157-0203
- Voigt T, von Eynatten H, Kley J (2009) Kommentar zu “Nördliche Harzrandstörung: Diskussionsbeiträge zu Tiefenstruktur, Zeitlichkeit und Kinematik” von V Wrede (*Z Dt Ges Geowiss* 159(2):293–316). [Comment on ‘The northern border fault of the Harz Mountains—contributions to the discussion on deep structure, timing and kinematics by V Wrede (*Z Dt Ges Geowiss* 159(2):293–316).] *Z Dt Ges Geowiss* 160:93–99. doi:10.1127/1860-1804/2009/0160-0093
- von Eynatten H, Voigt T, Meier A, Franzke H-J, Gaupp R (2008) Provenance of the clastic Cretaceous Subhercynian Basin fill: constraints to exhumation of the Harz Mountains and the timing of inversion tectonics in the Central European Basin. *Int J Earth Sci* 97:1315–1330. doi:10.1007/s00531-007-0212-0
- von Eynatten H, Dunkl I, Brix M, Hoffmann V-E, Raab M, Thomson SN, Voigt T (2016) Die oberkretazische Heraushebung des Harzes: thermochronologische und sedimentgeologische Daten. *Göttingen Contrib Geosci* 78:38–39
- White NJ, Jackson JA, McKenzie DP (1986) The relationship between the geometry of normal faults and that of the sedimentary layers in their hangingwalls. *J Struct Geol* 8:897–909. doi:10.1016/0191-8141(86)90035-0

- Withjack MO, Peterson ET (1993) Prediction of normal-fault geometries; a sensitivity analysis. *Am Assoc Pet Geol B* 77:18601873
- Wrede V (1988) Der nördliche Harzrand—flache Abscherbahn oder wrench-fault-system? *Geol Rundsch* 77(1):101–114. doi:10.1007/BF01848678
- Wrede V (2008) Nördliche Harzrandstörung: Diskussionsbeiträge zu Tiefenstruktur, Zeitlichkeit und Kinematik. *Z Dt Ges Geowiss* 159(2):293–316. doi:10.1127/1860-1804/2008/0159-0293
- Xiao H, Suppe J (1992) Origin of rollover. *Am Assoc Pet Geol B* 76:509–529
- Yamada Y, McClay K (2003a) Application of geometric models to inverted listric fault systems in sandbox experiments. Paper 1: 2D hanging wall deformation and section restoration. *J Struct Geol* 25(9):1551–1560. doi:10.1016/S0191-8141(02)00181-5
- Yamada Y, McClay K (2003b) Application of geometric models to inverted listric fault systems in sandbox experiments. Paper 2: insights for possible along strike migration of material during 3D hanging wall deformation. *J Struct Geol* 25(9):1331–1336. doi:10.1016/S0191-8141(02)00160-8
- Yegorova TP, Kozlenko VG, Pavlenkova NI, Starostenko VI (1995) 3-D density model for the lithosphere of Europe: construction method and preliminary results. *Geophys J Int* 121:873–892. doi:10.1111/j.1365-246X.1995.tb06445.x
- Ziesch J, Tanner DC, Krawczyk CM (2014) Strain associated with the fault-parallel flow algorithm during kinematic fault displacement. *Math Geosci* 46(1):59–73. doi:10.1007/s11004-013-9464-3